Macromolecules
ARTICLE

Macromolecules **2009**, *42*, 8977–8982 **8977**
DOI: 10.1021/ma9017235

Old Silks Endowed with New Properties

Gustavo R. Plaza,*,† Paola Corsini,‡ Enrico Marsano,‡ José Pérez-Rigueiro,† Lautaro Biancotto,† Manuel Elices,† Christian Riekel,§ Fernando Agulló-Rueda,∥ Eva Gallardo,⊥ José M. Calleja,⊥ and Gustavo V. Guinea†

†*Departamento de Ciencia de Materiales, ETSI Caminos, Canales y Puertos, Universidad Politécnica de Madrid, 28040 Madrid, Spain,* ‡*Dipartimento di Chimica e Chimica Industriale, Università di Genova, Via Dodecaneso 31-16146 Genova, Italy,* §*European Synchroton Radiation Facility, B.P. 220, F-38043, Grenoble Cedex, France,* ∥*Instituto de Ciencia de Materiales de Madrid, CSIC, 28049 Madrid, Spain, and* ⊥*Departamento de Física de Materiales, Universidad Autónoma de Madrid, 28049 Madrid, Spain*

Received August 2, 2009; Revised Manuscript Received September 18, 2009

ABSTRACT: High-performance regenerated silkworm *Bombyx mori* silk fibers with new properties that mimic those of spider silk can be produced through a wet spinning process modified with an immersion postspinning drawing (IPSD) step. IPSD fibers show the ability to recover from irreversible deformation, and their tensile behavior can be tailored repeatedly, features solely exhibited until now by natural spider silk. It is further shown that the new properties emerge from a microstructure that is closer to that of spider than to natural silkworm silk. This work demonstrates that processing plays a role at least comparable to that of the amino acid sequence in the final properties of the material. The spinning process does not only modify the mechanical parameters of the fiber but also can even prompt the emergence of new properties, opening a wide range of new applications for regenerated silk fibers. It also represents a significant change of the paradigm in the field of biomimetics, given that it relaxes the condition of copying the natural protein sequences as close as possible to recover the outstanding properties of the natural materials.

1. Introduction

After 400 million years of evolution,[1] nature has endowed silk fibers with outstanding mechanical properties such as high tensile strength, large deformation at breaking, and an unbeatable capacity for absorbing energy not surpassed by synthetic fibers. Natural silks are the result of an optimized balance between composition and processing that provides every species with a fiber tailored to their needs; silkworm silk is stiff and elastic with a high-yield stress (> 200 MPa) suitable to protect the pupa during its metamorphosis to an adult moth. Silks secreted by the major ampullate gland of spiders (MA silk) are tough and best suited to absorb and dissipate the energy of a prey impinging at the web, being also able to recover the original mechanical properties after wetting and subsequent drying.

The exquisite adaption of silk fibers to their distinct biological functions has been customarily attributed to the presence of specialized proteins (known as fibroins), originated from gene sequences extremely conserved along evolution. The strength of *Bombyx mori* (silkworm) silk has been directly related to the presence of β-sheet nanocrystallites,[2,3] which appear as the result of piling up β-pleated sheets formed by the motif $(GAGAGS)_n$.[4] Major ampullate fibroins from araneoids show, in opposition, stable repeats A_n, GA, GGX, and $GPG(X)_n$[5] that have been related to the distinct features of spider silk not found in silkworm silk, such as supercontraction.[6,7]

Consequently, attempts to mimic the outstanding properties of silks have been primarily oriented toward copying the protein sequences, overlooking more or less explicitly the influence of the spinning process.[8,9] Several organisms were used in expressing spider silk proteins from synthetic genes containing amino acid sequence motifs expected to be related to the mechanical performance of silks. Microorganisms such as bacteria[10] and yeast[11−13] are prevalent, although insect and mammalian systems have also been proposed.[12,13] This strategy, however, did not produce the expected results because values of tensile strength and elongation at rupture are significantly lower than those of natural spider silks.[13] The reasons for such results are still controversial, and the smaller size of the cloned proteins (∼1/3 of natural, at most) might have a definite effect on them as well as the oversimplified conditions under which fibers are spun and processed.

To reduce the number of variables while keeping in focus the role of processing, regeneration of natural silk has come out as an alternative approach. This route has been mainly explored with *Bombyx mori* silk because of the feasibility of obtaining large amounts of natural material in comparison with the small quantities of spider silk available, even if forced silking techniques are used.[14−20] Because regenerated fibers have a composition closer to that of the natural silks, differences between the natural and the regenerated fibers should rely more on the spinning process than on composition. It has been found that variations of the spinning conditions can be associated with the tensile properties of the fiber,[20,21] showing that the same composition may yield different mechanical behavior under different processing conditions. Work on regenerated silkworm fibers has usually yielded values of tensile strength and, particularly, deformation at breaking far below the values of natural silkworm silk, probably because of the drastic simplifications ordinarily introduced in processing compared with the natural systems. Recently, new processing techniques have produced regenerated fibers with strength close to that of natural ones.[22−24]

Here we go a step further to show how spinning conditions not only control the mechanical parameters of silk fibers but prompt the appearance of new properties not even shown by the natural silk. This work reports a procedure that uses a step within the

*Corresponding author. E-mail: gplaza@mater.upm.es.

Published on Web 10/02/2009

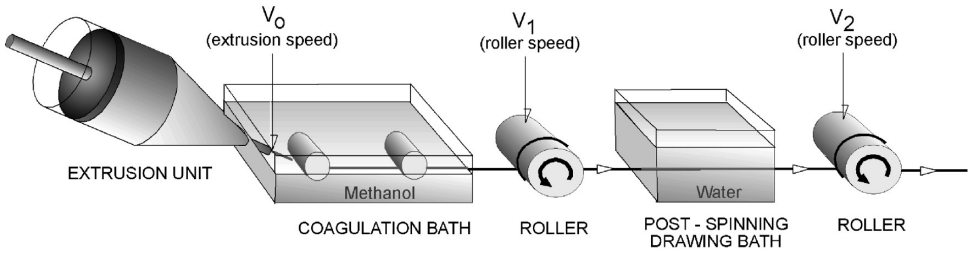

Figure 1. Scheme of the spinning process of regenerated IPSD fibers. The different velocities defined in the text are illustrated.

usual wet spinning technique, which we designate immersion postspinning drawing (IPSD). The procedure leads to regenerated fibers that are more ductile than natural ones and with toughness similar to that of natural silkworm silks.

2. Experimental Section

Regenerated silk fibroin fibers were prepared as previously described.[24] Freeze-dried highly porous material based on *Bombyx mori* silk fibroin was prepared, and it was dispersed into a commercial aqueous solution of NMMO−H_2O (50/50 w/w). The dispersion was concentrated under vacuum at 55 °C to obtain NMMO hydrates with the desired water content (the maximum value was ca. 12.8%, w/w) to dissolve silk fibroin. The water content was determined by the Karl Fischer method. Silk fibroin concentration was fixed to 17% (w/w) with respect to the solution.

To prepare silk fibroin solutions in NMMO hydrates, the dispersion was heated to 110 °C for 20 min in a homemade heater. The solutions were stirred under a nitrogen atmosphere, controlling time by time the progress of dissolution with an optical microscope. Air bubbles were trapped in the silk fibroin solutions because of the fast energetic stirring, so centrifugation at high temperature of the dope before spinning was required to disengage them. During the dissolution and the spinning of solutions, no marked polymer degradation was observed.

Silk fibroin solutions were spun with a dry-jet wet spinning line composed of an extrusion unit, a coagulation bath, a take up, an IPSD bath, which consists of a bath of water in which the spun fiber is subjected to postspinning drawing, and finally a collecting spool, called roller, as shown in Figure 1. The introduction of the postspinning drawing bath is original to this work and is based on previous studies on the influence of water on the properties of regenerated silk fibers performed by the authors.[21,22] Silk fibroin solutions were extruded at 90 °C and at fixed rate V_0 = 4m/min through a 100 μm hole spinneret with 50 mm of air gap into a coagulation bath of methanol. The coagulated thread was further stretched in the IPSD bath and finally collected on the roller. The collecting rate could be varied so that fibers were spun with different draw ratios. In this work, we used samples with V_1/V_0 = 0.2, where V_1 is the velocity of the take-up spool speed (Figure 1), and V_2/V_1 = 7.2, where V_2 is the roller speed. These values were chosen after a preliminary screening because of the high tensile properties in terms of tensile strength and strain at breaking exhibited by the fibers. Nevertheless, other important properties such as adaptability or recovery were also shown by samples spun under other postspinning drawing ratios.

To measure the mechanical properties, regenerated silk fibroin fibers were mounted on perforated cardboard cards. Each sample was glued across a rectangular hole to give a gauge length of 25 mm, as shown elsewhere.[25] The support was mounted in an Instron 4411 tensile testing machine, after which the cardboard frame was cut so that the entire load was transmitted through the fiber. An electronic balance (AND 1200G; resolution 0.1 mgf) under the lower grip was used instead of a conventional load cell to measure force. The crosshead was moved with a constant and fixed rate equal to 2 mm/min, and the measurements were performed at 25 °C and 35% relative humidity.

The supercontraction process proceeded as described elsewhere:[26] The initial length of the samples was the maximum length at which the fiber was taut but not subjected to load. From this position, the upper grip was lowered to ~50% of the initial length, and the fiber was immersed in water. Water was removed after 24 h, and the fiber was allowed to dry overnight. The supercontracted length was established as the length at which the fiber was taut, but no load was measured from the balance. Tensile testing proceeded by moving the crosshead at a constant and fixed rate of 1 mm/min. Temperature and relative humidity for all tests were 25 °C and 35%, respectively.

To measure the diameters, two small pieces, 5 mm long, adjacent to both sides of each sample were retrieved, metallized with gold, and observed in a scanning electron microscope (SEM-JEOL 6300). The samples were observed at 10 kV. Diameters at a given section of the fiber were calculated as the average of at least 10 measurements on each micrograph, and the cross-sectional area was computed assuming a circular cross-section. The cross-sectional areas were used to rescale force displacement plots into true stress−true strain curves. True stresses and true strains were calculated under the hypothesis of constant volume during deformation, a usual hypothesis with silkworm silk[25] that has been proven for spider silk.[27] We calculated the cross-sectional area of the supercontracted fiber after proving that volume was conserved during supercontraction by measuring the diameter of fibers subjected to supercontraction and comparing them with the diameter of adjacent fibers not subjected to supercontraction. Elastic modulus (E), tensile strength (σ_u), and elongation at break (ε_u) were obtained from the stress−strain curves.

To determine microstructural parameters, synchrotron radiation (SR) microdiffraction experiments were performed at the ESRF-ID13 beamline using an ~1 × 1 μm^2 monochromatic beam from crossed mirrors at a wavelength of 0.09614 nm.[28] Short fiber sections were glued to O-rings attached to glass capillaries that were fixed via Hampton magnetic supports to a magnetic base on a motorized translation stage. Linear scans of fiber sections through the beam were carried out to probe local structural changes. A FreLon CCD camera[29] with a microchannel-plate image intensifier, 2K × 2K pixels, and 16-bit readout was used for data collection. Data collection times were typically 5−15 s/pattern. The detector-to-sample distance was calibrated with Al_2O_3 powder to 92.5 mm. The samples were aligned in the X-ray beam by an on-axis microscope, which was calibrated to the focal spot. Data analysis was performed with the FIT2D program.[30] Patterns recorded outside a fiber during a scan were used for background correction. Reflection profiles were azimuthally or radially integrated and fitted by Gaussian profiles.[31] A zero-order polynomial was assumed for diffuse sample background scattering. We estimated the crystallinity of the fibers by separating the Bragg reflections from the short-range order background.[28] We integrated the patterns azimuthally through 360° and fitted the radial profile by narrow Bragg peaks corresponding to the crystalline nanodomains, a broad peak because of the short-range-order background and a zero-order polynomial for residual diffuse sample scattering.

To measure the molecular alignment along the fiber axis, we collected micro-Raman spectra of the as-spun and the contracted regenerated fibers using an Ar-ion-laser-pumped Ti−sapphire

laser at 783 nm to avoid fluorescence emission from the sample and a double grating spectrometer with a CCD detector. Light was focused to and collected from the fiber with a 50× microscope objective. Each sample has been analyzed in several points, and no sign of structural deterioration was observed under experimental conditions. Polarized spectra were collected, where the incident and scattered light are either parallel (I_{zz}) or perpendicular (I_{xx}) to the fiber axis (z direction). We have chosen the spectral range between 1100 and 1800 cm^{-1}, which contains the amide III and amide I bands. They arise, respectively, from vibrations approximately parallel and perpendicular to the polypeptide backbone, and their intensity in polarized spectra is very sensitive to the degree of orientation of the β-sheet crystallites.[32]

The nanostructural organization of the fibers was observed by means of atomic force microscopy. The preparation of the samples has been described elsewhere.[33] In brief, fibers were embedded in Spurr's resin and allowed to cure for 72 h at 70 °C. The function of the Spurr's resin is to serve as a mechanical support to the fiber during the ultramicrotomy step. The longitudinal sections were obtained by ultramicrotomy with a diamond blade. A Bermad 2000 AFM (Nanotec Electrónica, Spain) was used to obtain the atomic force microscopy images. Olympus OMCL RC800PSA cantilevers were used for the observation, and the highest resolution was obtained with the stiffest tip (nominal stiffness 0.76 N/m). AFM images were recorded in the dynamic mode in the repulsive regime of the tip−sample interaction.[34] The processing of the AFM images has been performed with the WSxM program (Nanotec, Spain).[35] Processing has consisted of simple equalizing and adjusting the contrast and the brightness of the micrographs. No filter has been used to improve the quality of the images or to highlight their details.

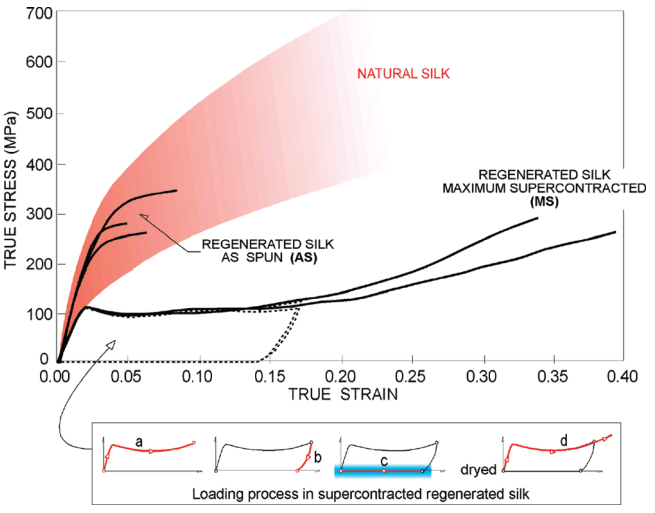

Figure 2. Stress−strain curves of IPSD fibers under the as-spun condition (AS) and after maximum supercontraction (MS). The ratio between the length of MS fiber compared with that of the initial AS fiber yields a value of $L/L_0 = 0.76 \pm 0.02$, which corresponds to a contraction of 24%. The range of tensile properties exhibited by natural *Bombyx mori* silk fibers is shown to allow comparison. The dotted lines correspond to a recovery test on the previously supercontracted fibers. The recovery test consists of stretching the supercontrated fiber to a given strain (in this case $\varepsilon = 0.18$) and subjecting the fiber to a new maximum supercontraction step, as illustrated in the inset.

3. Results and Discussion

Regenerated fibers were spun through a conventional wet spinning procedure[24] in which an additional step known as immersion post spinning drawing (IPSD) was performed. The introduction of the postspinning drawing bath as an intrinsic part of the spinning process is original to this work and is based on previous studies on the influence of water on the properties of regenerated silk fibers carried out by the authors.[21,22]

Figure 2 shows the stress−strain curves of IPSD fibers as spun (AS). The range of stress−strain curves of natural silkworm silk fibers[25] is indicated. The elastic modulus of the AS fibers lies within the range observed in natural fibers, as shown in Table 1. Although the tensile strength and the strain at breaking improve significantly compared with previous values of fibers subjected to postspinning drawing in air,[22] they still lie below those of the natural material. Consequently, the work of fracture does not reach the outstanding values of natural silkworm silk.

The tensile properties of IPSD fibers are largely modified if subjected to supercontraction, as shown in Figure 2. The term supercontraction describes a significant reduction in the length of spider silk fibers in humid environments.[36] Although the biological function of supercontraction is still under debate,[36−38] it has been found that supercontraction is one of the distinct features of the silk spun by the major ampullate gland (MA silk) of spiders, which distinguishes it clearly from the silks of other species, such as silkworms, which do not show an equivalent effect.[39]

The study of the supercontraction effect in MA spider silk has allowed the identification of the maximum supercontracted (MS) state[40] as a ground state, which can be always reached independently from the condition of the material and the presence of irreversible strains by simply subjecting the unrestrained fiber to water immersion and subsequent drying, a property labeled as recovery.[26] It has also been found that the MS state can be used as the base state from which the tensile properties of spider silk can be tailored in a reproducible way,[41,42] a property that allows the spider to adapt the fiber's properties to its immediate requirements.[43] Consequently, recovery and adaptability arose as specific features of MA spider silks not shared by the silks of other organisms and distinguish supercontraction in spider from the contraction shown by other polymeric fibers. For instance, although regenerated silkworm silk fibers show a modest contraction when wetted,[21] this effect has not been labeled as supercontraction because it was not related to the existence of a basal state independent from the previous conditions of the sample.

After being allowed to supercontract, IPSD fibers yield a reduction in length of $L/L_0 = 0.76 \pm 0.02$, where L_0 is the initial length and L is the length after contraction, corresponding to a contraction of 24%. The existence of a true maximum supercontracted state in IPSD fibers is shown by the recovery of the fibers illustrated in Figure 2. The concurrence among the original MS curves prior to and after the first stretching step indicates that the IPSD fibers can recover from irreversible deformations and that there is a ground state that can be reached independently from the previous loading history of the fiber. Consequently, the

Table 1. Comparison of the Tensile Properties of As-Spun (AS) Regenerated Silk Fibroin Fibers, Maximum Supercontracted (MS) Regenerated Silk Fibroin Fibers, *Argiope trifasciata* Spider Silk,[48] and *Bombyx mori* Silkworm Silk[25,a]

	D (μm)	E (GPa)	ε_u (%)	σ_u (MPa)	W_f (MPa/m^3)
AS regenerated silk fibroin	41 ± 4	12.2 ± 0.3	6 ± 1	320 ± 20	13 ± 2
MS regenerated silk fibroin	47 ± 5	6.8 ± 0.3	34 ± 1	273 ± 6	52 ± 2
MA silk, *Argiope trifasciata*	6.6 ± 0.2	6.9 ± 0.4	26 ± 2	780 ± 50	90 ± 10
Bombyx mori	11.5 ± 0.2	9−17	0.15 to 0.27	400−700	50−60

[a] True stress and true strain were calculated from the data presented in the references.

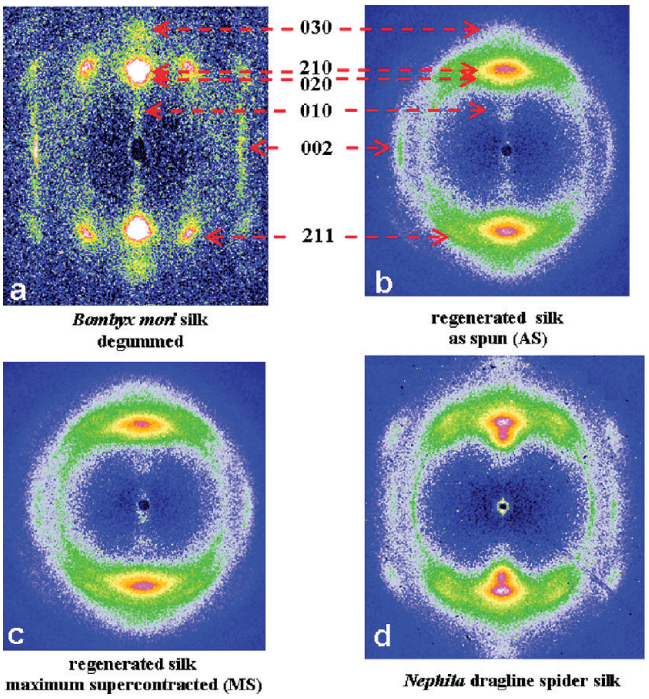

Figure 3. X-ray diffraction diagrams of regenerated silk under (b) the AS condition and (c) the MS condition. Comparison with the diagram of (a) natural *Bombyx mori* silk indicates that the spots in the diagrams of the regenerated fibers can be assigned to the same reflections found in the natural material. The diffraction pattern from *Nephila senigalensis* MAS fiber (d, adapted from previous work[44]) shows a similar chain alignment as *Bombyx mori* silk.

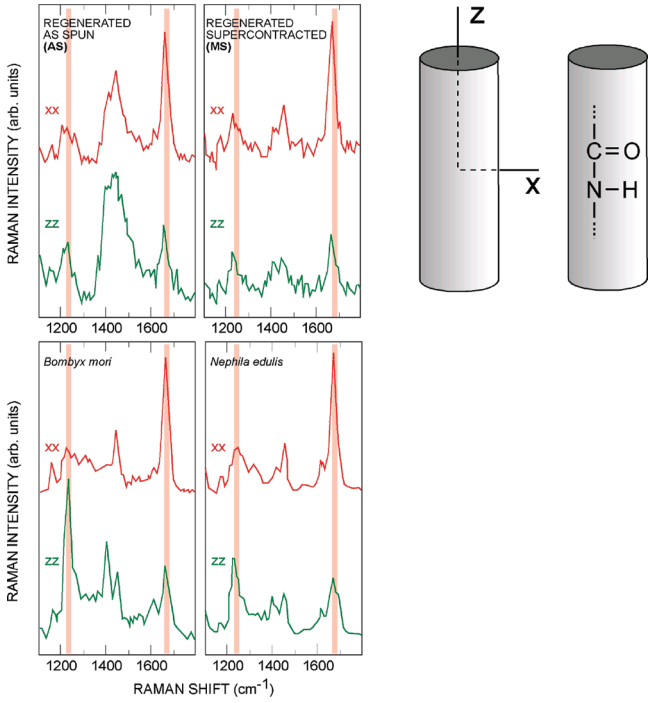

Figure 4. MicroRaman spectra of the regenerated silk in the AS and in the MS condition. Spectra of natural *Bombyx mori* silk and spider (*Nephila edulis*) are shown for comparison. The peaks corresponding to the vibration modes amide I and amide III are highlighted. The inset illustrates the orientation of the axes with respect to the fiber.

effect of water on the unrestrained IPSD regenerated fibers can be labeled properly as supercontraction.[26]

The differences of the tensile properties of MS regenerated fibers with those of natural silkworm silk and their similarities with spider silk illustrated in Figure 2 and in Table 1 require exploration of whether this behavior can be explained by the different microstructures of the silks. The microstructures of the regenerated silkworm silk and natural silkworm and spider silk fibers have been compared by X-ray diffraction, Raman spectroscopy, and atomic force microscopy.

The X-ray diffraction patterns of regenerated fibers under as-spun (AS) and maximum supercontrated (MS) conditions, natural *Bombyx mori* fibers, and spider MA silk fibers are shown in Figure 3. AS, MS, and natural *B. mori* patterns show the same reflections as those that can be indexed for the same orthorhombic unit cell[2] (Figure 3a−c). The orientation of the equatorial 210 reflection indicates that the local fiber axis is oriented along the macroscopic fiber axis.

Analysis of the azimuthal intensity profile of the 210 reflection[31] gives the orientation distribution of the polymer chains in the crystalline nanodomains. The width of the narrow component has a value of 23 and 28.5° for the AS and MS regenerated fibers, respectively. Natural *Bombyx mori* silk fibers show a higher chain alignment with an azimuthal 210 width of 14.1° fwhm. A similar azimuthal width was observed for spider silk at orb weaving extrusion speed,[44] as can be seen in the *Nephila* dragline silk pattern in Figure 3d.[44] The nanodomains slightly lose their alignment along the fiber axis during supercontraction of the regenerated fibers, as shown by the increase in the width from the AS to the MS samples. It has been found that supercontraction of spider silk also results in a large increase in azimuthal width for the equatorial reflections.[45] The degree of orientation of the crystalline fraction is determined from the azimuthal broadening of the equatorial 210/100 reflections.[31]

f_c values show the same trend as the azimuthal width (AS: 0.85; MS: 0.79; *B. mori*: ∼0.96; MAS spider silk: 0.96).

From the radial profile of the 010/210 reflections, particle sizes in the nanometer range were obtained (AS: 3.0 nm; MS: 2.7 nm; *B. mori*: 4.2 nm; MAS spider silk: 3.3 nm). These dimensions are similar to nanodomains observed for natural *Bombyx mori*,[28] although a significantly larger dimension along the hydrogen-bonded [210] direction as that for natural *Bombyx mori* silk is not observed.

The crystallinity of the AS regenerated fiber was estimated to be 20% and remained unchanged for the MS fiber. The degree of crystallinity of regenerated fibers lies between that of spider silk (10−15%)[46] and that of natural *Bombyx mori* silk fibers, (56−65%).[3,28]

The Raman spectra for I_{xx} and I_{zz} polarization configurations for regenerated fibers as spun (AS) and maximum supercontracted (MS), natural *Bombyx mori*,[20] and MAS spider silk[32] are shown in Figure 4. The band at 1230 cm^{-1} corresponds to the amide III vibration, which is stronger for I_{zz} because it corresponds to protein chains oriented preferably along the fiber axis. The amide I band (1660 cm^{-1}), on the contrary, involves mostly a C═O stretching perpendicular to the peptide bond direction and is stronger for I_{xx}. To quantify the degree of orientation of protein chains, we propose the empirical parameter $p = I_{zz}$(amide III)/I_{zz}(amide I). This has the advantage over other parameters that a single measurement is needed, eliminating any scaling among different measurements. p increases with the degree of ordering and is 2.5 for the natural *Bombyx mori*, 1.2 for the as-spun regenerated, 1.0 for the supercontracted regenerated, and 0.7 for MAS spider silk.

Observation by atomic force microscopy of regenerated silk fibroin fibers in the as-spun (AS) and maximum supercontracted (MS) conditions has shown that both samples are homogeneous on a micrometer scale, with no skin-core organization, a result supported by X-ray diffraction data. High-resolution AFM images of regenerated fibers as well

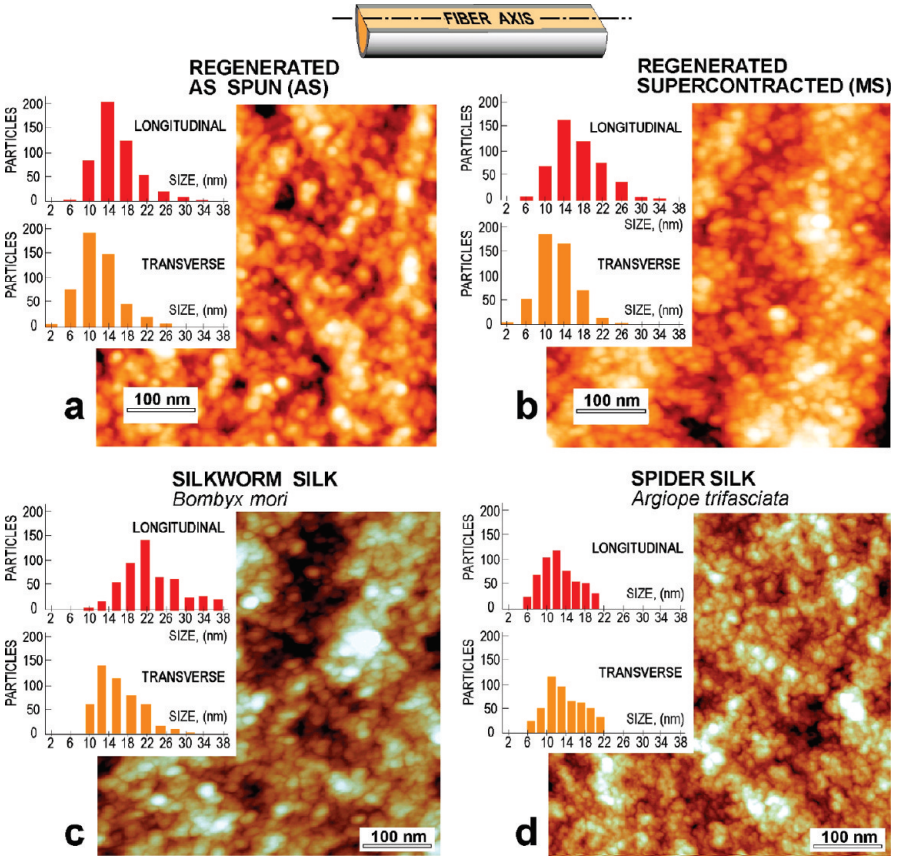

Figure 5. AFM micrographs of the regenerated silk in (a) the AS condition and (b) the MS condition of longitudinal sections of the fibers. AFM micrographs of *Bombyx mori* and MAS spider (*Argiope trifasciata*) silk are shown for comparison. The histograms show the size of the nanoglobules, which are approximated by ellipses with a major and minor axis. As illustrated in the inset, each micrograph is oriented so that the axis of the fiber lies on the horizontal direction.

as *B. mori* silkworm silk and MAS spider silk are shown in Figure 5.

Both AS and MS fibers show the usual nanoglobular structure found in natural[33] and regenerated silk fibers.[47] The nanoglobules of the AS fiber yield values of 16 ± 5 and 12 ± 4 nm for the major and minor axis, with a maximum size of 34 nm. The nanoglobules in the MS sample yield values of 17 ± 6 and 13 ± 4 nm, with a maximum size of 34 nm, very similar to those of the AS sample.

The results above show that regenerated *Bombyx mori* fibers subjected to IPSD display features that were thought to be exclusive to natural MA spider silk and which are not exhibited by their natural precursors. The microstructural analysis shows that IPSD fibers resemble the microstructure of MA spider silk in their basic aspects (crystalline fraction, size of the nanocrystals, orientation of the peptide bonds, and size and degree of anisotropy of the nanoglobules), clearly different from that of silkworm silk.

Obtaining a modified microstructure closer to that exhibited by spider silk fibers is most probably at the base of the new properties displayed by IPSD fibers, in contrast with their natural precursor. The existence of supercontraction implies that the movement of the molecular chains is not sufficiently restrained so as to avoid coiling due to elastomeric effects. The lower orientation of the protein chains in MS compared with that of AS samples and the absence of changes in the crystalline fraction, in the size of the crystalline nanodomains, or in the overall nanoglobular organization indicate that the coiling of the elastomeric chains is accompanied by the rotation of the nanocrystals. Compared with IPSD regenerated fibers, the highly crystalline and oriented microstructure of natural silkworm silk fibers would represent a major constraint to these movements, which explains the absence of the supercontraction effect in the natural material, but a microstructure of lesser crystallinity and orientation would not represent such a stringent constraint.

4. Conclusions

Spinning conditions are shown to be essential for determining the mechanical properties of regenerated silkworm silk fibers in a higher degree than expected because they not only modify the stiffness, ductility, and strength of the fiber but also can even prompt the emergence of new properties.

The results shown here demonstrate that IPSD endows regenerated silkworm silk fibers with the ability to supercontract and recover. Consequently, it would make it possible to control their molecular alignment by methods similar to those applied to spider silk[41] and lead to very different mechanical conditions in a very repeatable and accurate way. The new properties open a wide range of applications of regenerated silk fibers, especially for those where a given, repetitive, mechanical behavior is sought.

Acknowledgment. We would like to thank Mario Traverso for his helpful work on the wet-spinning line and Dr. G. Freddi (Stazione Sperimentale per la Seta, Milan, Italy) for providing silkworm silk fibroin. In addition, Dr. Charlotte Vendrely helped with the experimental setup of the X-ray diffraction experiments. Ultramicrotomy was performed by E. Baldonedo (Centro de Microscopía Electrónica, Universidad Complutense de Madrid, Spain). Dr. A. Gil (Nanotec Electrónica S.L., Madrid, Spain) offered support for the AFM observations. We are grateful to José Miguel Martínez for his help with the artwork. The work was funded by Ministerio de Educación y Ciencia (Spain) through

project MAT 2006-04387. The financial support from the Comunidad de Madrid (Spain) to carry out this investigation through the MADR.IB-CM/S-SAL/0312/2006 program is gratefully acknowledged.

References and Notes

(1) Craig, C. L. *Annu. Rev. Entomol.* **1997**, *1*, 231–267.
(2) Marsh, R. E.; Corey, R. B.; Pauling, L. *Biochim. Biophys. Acta* **1955**, *1*, 1–34.
(3) Kaplan, D. L.; Lombardi, S.; Muller, W. S.; Fossey, S. A. *Biomaterials: Novel Materials from Biological Sources*; Stockton Press: New York, 1991; p 53.
(4) Xia, Q. Y.; Zhou, Z. Y.; Lu, C.; Cheng, D. J.; Dai, F. Y.; Li, B.; Zhao, P.; Zha, X. F.; Cheng, T. C.; Chai, C. L.; Pan, G. Q.; Xu, J. S.; Liu, C.; Lin, Y.; Qian, J. F.; Hou, Y.; Wu, Z. L.; Li, G. R.; Pan, M. H.; Li, C. F.; Shen, Y. H.; Lan, X. Q.; Yuan, L. W.; Li, T.; Xu, H. F.; Yang, G. W.; Wan, Y. J.; Zhu, Y.; Yu, M. D.; Shen, W. D.; Wu, D. Y.; Xiang, Z. H.; Yu, J.; Wang, J.; Li, R. Q.; Shi, J. P.; Li, H.; Li, G. Y.; Su, J. N.; Wang, X. L.; Li, G. Q.; Zhang, Z. J.; Wu, Q. F.; Li, J.; Zhang, Q. P.; Wei, N.; Xu, J. Z.; Sun, H. B.; Dong, L.; Liu, D. Y.; Zhao, S. L.; Zhao, X. L.; Meng, Q. S.; Lan, F. D.; Huang, X. G.; Li, Y. Z.; Fang, L.; Li, C. F.; Li, D. W.; Sun, Y. Q.; Zhang, Z. P.; Yang, Z.; Huang, Y. Q.; Xi, Y.; Qi, Q. H.; He, D. D.; Huang, H. Y.; Zhang, X. W.; Wang, Z. Q.; Li, W. J.; Cao, Y. Z.; Yu, Y. P.; Yu, H.; Li, J. H.; Ye, J. H.; Chen, H.; Zhou, Y.; Liu, B.; Wang, J.; Ye, J.; Ji, H.; Li, S. T.; Ni, P. X.; Zhang, J. G.; Zhang, Y.; Zheng, H. K.; Mao, B. Y.; Wang, W.; Ye, C.; Li, S. G.; Wang, J.; Wong, G. K. S.; Yang, H. M. *Science* **2004**, *5703*, 1937–1940.
(5) Gatesy, J.; Hayashi, C.; Motriuk, D.; Woods, J.; Lewis, R. *Science* **2001**, *5513*, 2603–2605.
(6) Work, R. W. *Trans. Am. Microsc. Soc.* **1977**, *2*, 170–189.
(7) Lewis, R. V. *Chem. Rev.* **2006**, *9*, 3762–3774.
(8) Teule, F.; Furin, W. A.; Cooper, A. R.; Duncan, J. R.; Lewis, R. V. *J. Mater. Sci.* **2007**, *21*, 8974–8985.
(9) Hardy, J. G.; Romer, L. M.; Scheibel, T. R. *Polymer* **2008**, *20*, 4309–4327.
(10) Prince, J. T.; Mcgrath, K. P.; Digirolamo, C. M.; Kaplan, D. L. *Biochemistry* **1995**, *34*, 10879–10885.
(11) Fukushima, Y. *Biopolymers* **1998**, *4*, 269–279.
(12) Huemmerich, D.; Scheibel, T.; Vollrath, F.; Cohen, S.; Gat, U.; Ittah, S. *Curr. Biol.* **2004**, *22*, 2070–2074.
(13) Lazaris, A.; Arcidiacono, S.; Huang, Y.; Zhou, J. F.; Duguay, F.; Chretien, N.; Welsh, E. A.; Soares, J. W.; Karatzas, C. N. *Science* **2002**, *5554*, 472–476.
(14) Matsumoto, K.; Uejima, H.; Iwasaki, T.; Sano, Y.; Sumino, H. *J. Appl. Polym. Sci.* **1996**, *4*, 503–511.
(15) Trabbic, K. A.; Yager, P. *Macromolecules* **1998**, *2*, 462–471.
(16) Liivak, O.; Blye, A.; Shah, N.; Jelinski, L. W. *Macromolecules* **1998**, *9*, 2947–2951.
(17) Um, I. C.; Ki, C. S.; Kweon, H. Y.; Lee, K. G.; Ihm, D. W.; Park, Y. H. *Int. J. Biol. Macromol.* **2004**, *1*−*2*, 107–119.
(18) Ha, S. W.; Tonelli, A. E.; Hudson, S. M. *Biomacromolecules* **2005**, *3*, 1722–1731.
(19) Xie, F.; Zhang, H. H.; Shao, H. L.; Hu, X. C. *Int. J. Biol. Macromol.* **2006**, *3*−*5*, 284–288.
(20) Corsini, P.; Perez-Rigueiro, J.; Guinea, G. V.; Plaza, G. R.; Elices, M.; Marsano, E.; Carnasciali, M. M.; Freddi, G. *J. Polym. Sci., Part B: Polym. Phys.* **2007**, 2568–2579.
(21) Plaza, G. R.; Corsini, P.; Perez-Rigueiro, J.; Marsano, E.; Guinea, G. V.; Elices, M. *J. Appl. Polym. Sci.* **2008**, *3*, 1793–1801.
(22) Corsini, P. *New Fibres Based on Natural Polymers: Silk and Cellulose*. Ph.D. Thesis, Universita degli Studi di Genova, Genova, 2008.
(23) Zhu, Z. H.; Ohgo, K.; Asakura, T. *eXPRESS Polym. Lett.* **2008**, *12*, 885–889.
(24) Marsano, E.; Corsini, P.; Arosio, C.; Boschi, A.; Mormino, M.; Freddi, G. *Int. J. Biol. Macromol.* **2005**, *4*, 179–188.
(25) Perez-Rigueiro, J.; Viney, C.; Llorca, J.; Elices, M. *J. Appl. Polym. Sci.* **1998**, *12*, 2439–2447.
(26) Elices, M.; Perez-Rigueiro, J.; Plaza, G.; Guinea, G. V. *J. Appl. Polym. Sci.* **2004**, *6*, 3537–3541.
(27) Guinea, G. V.; Perez-Rigueiro, J.; Plaza, G. R.; Elices, M. *Biomacromolecules* **2006**, *7*, 2173–2177.
(28) Martel, A.; Burghammer, M.; Davies, R. J.; Riekel, C. *Biomacromolecules* **2007**, 3548–3556.
(29) Labiche, J. C.; Mathon, O.; Pascarelli, S.; Newton, M. A.; Ferre, G. G.; Curfs, C.; Vaughan, G.; Homs, A.; Carreiras, D. F. *Rev. Sci. Instrum.* **2007**, *78*, 091301.
(30) Hammersley, A. P.; Brown, K.; Burmeister, W.; Claustre, L.; Gonzalez, A.; McSweeney, S.; Mitchell, E.; Moy, J. P.; Svensson, S. O.; Thompson, A. W. *J. Syn. Rad.* **1997**, *4*, 67–77.
(31) Riekel, C.; Branden, C.; Craig, C.; Ferrero, C.; Heidelbach, F.; Muller, M. *Int. J. Biol. Macromol.* **1999**, *2*−*3*, 179–186.
(32) Rousseau, M. E.; Lefevre, T.; Beaulieu, L.; Asakura, T.; Pezolet, M. *Biomacromolecules* **2004**, *6*, 2247–2257.
(33) Perez-Rigueiro, J.; Elices, M.; Plaza, G. R.; Guinea, G. V. *Macromolecules* **2007**, *15*, 5360–5365.
(34) Garcia, R.; San Paulo, A. *Phys. Rev. B* **1999**, *7*, 4961–4967.
(35) Horcas, I.; Fernandez, R.; Gomez-Rodriguez, J. M.; Colchero, J.; Gomez-Herrero, J.; Baro, A. M. *Rev. Sci. Instrum.* **2007**, 1.
(36) Work, R. W. *Text. Res. J.* **1977**, *10*, 650–662.
(37) Guinea, G. V.; Elices, M.; Perez-Rigueiro, J.; Plaza, G. *Polymer* **2003**, *19*, 5785–5788.
(38) Savage, K. N.; Guerette, P. A.; Gosline, J. M. *Biomacromolecules* **2004**, *3*, 675–679.
(39) Perez-Rigueiro, J.; Viney, C.; Llorca, J.; Elices, M. *Polymer* **2000**, *23*, 8433–8439.
(40) Perez-Rigueiro, J.; Elices, M.; Guinea, G. V. *Polymer* **2003**, *13*, 3733–3736.
(41) Guinea, G. V.; Elices, M.; Perez-Rigueiro, J.; Plaza, G. R. *J. Exp. Biol.* **2005**, *1*, 25–30.
(42) Elices, M.; Perez-Rigueiro, J.; Plaza, G. R.; Guinea, G. V. *JOM* **2005**, *2*, 60–66.
(43) Garrido, M. A.; Elices, M.; Viney, C.; Perez-Rigueiro, J. *Polymer* **2002**, *4*, 1537–1540.
(44) Riekel, C.; Vollrath, F. *Int. J. Biol. Macromol.* **2001**, *3*, 203–210.
(45) Grubb, D. T.; Ji, G. D. *Int. J. Biol. Macromol.* **1999**, *2*−*3*, 203–210.
(46) Yang, Z.; Grubb, D. T.; Jelinski, L. W. *Macromolecules* **1997**, *26*, 8254–8261.
(47) Perez-Rigueiro, J.; Biancotto, L.; Corsini, P.; Marsano, E.; Elices, M.; Plaza, G. R.; Guinea, G. V. *Int. J. Biol. Macromol.* **2009**, *2*, 195–202.
(48) Perez-Riguero, J.; Elices, M.; Llorca, J.; Viney, C. *J. Appl. Polym. Sci.* **2001**, *9*, 2245–2251.